JETP Letters, Vol. 72, No. 11, 2000, pp. 583–592. Translated from Pis'ma v Zhurnal Éksperimental'noĭ i Teoreticheskoĭ Fiziki, Vol. 72, No. 11, 2000, pp. 845–858.

Microwave Response of High-T_c Superconducting Crystals: Results, Problems, and Prospects

M. R. Trunin

Institute of Solid State Physics, Russian Academy of Sciences, Chernogolovka, Moscow region, 142432 Russia
e-mail: trunin@issp.ac.ru

Received October 30, 2000

The results of studying temperature behavior of the microwave surface impedance $Z_s(T)$ and conductivity tensor $\hat{\sigma}(T)$ of high-T_c superconducting (HTSC) single crystals are analyzed. The emphasis is on the experimental facts that are inconsistent with the known electrodynamic concepts of conductivity mechanisms in these materials. Possible reasons for the inconsistency are discussed in the context of structural features of the HTSC crystals, and the outlook for future investigations is outlined. © *2000 MAIK "Nauka/Interperiodica".*

PACS numbers: 74.25.Nf; 74.72.-h; 74.20.De

INTRODUCTION

Despite a certain progress in elucidating the physical properties of high-temperature superconductors (HTSC), no consistent microscopic theory has been developed to date that would be capable of explaining the totality of available and firmly established experimental data even for a relatively narrow region of the phase diagram corresponding to optimum-doped HTSC materials and maximum critical temperatures T_c. A fundamental problem of type of superconducting interaction in HTSC also remains to be solved. There is much controversy over the symmetry of the order parameter, the mechanisms of quasiparticle relaxation, and the role of impurities and anisotropy in HTSC materials. Among the experimental methods of studying these problems are measurements of the linear microwave response of HTSC single crystals, i.e., studies of the temperature dependences of the surface impedance $Z_s(T) = R_s(T) + iX_s(T)$ and complex conductivity $\sigma(T) = \sigma'(T) - i\sigma''(T)$ at microwave (MW) frequencies and low (<0.1 Oe) amplitudes of ac field. It is known that the precise measurements of $Z_s(T)$ in classical superconductors proved to be quite informative: the gap Δ was derived from the temperature dependence of surface resistance $R_s(T) \propto e^{-\Delta/k_BT}$ at $T < T_c/2$, the field penetration depth $\lambda(T)$ into a superconductor was derived from the reactance $X_s(T) = \omega\mu_0\lambda(T)$ at $T < T_c$, and the electron mean free path was determined by measuring $R_s(T)$ and $X_s(T)$ in the normal state ($T \geq T_c$). The applicability of the Bardeen–Cooper–Schrieffer (BCS) theory [1] to classical superconductors was clearly demonstrated by the nonmonotonic behavior (coherence peak) of the microwave conductivity $\sigma'(T)$ at $0.8 < T/T_c \leq 1$. However, even the early studies of the impedance and conductivity of HTSC materials did not fit into the BCS theory: there was no coherence peak in $\sigma'(T)$ and, instead of exponential behavior at low temperatures, $Z_s(T)$ exhibited power law temperature dependence. A linear dependence of the penetration depth $\Delta\lambda_{ab}(T) \propto T$ at $T < 25$ K, first observed in 1993 in [2] for the *ab* plane of $YBa_2Cu_3O_{6.95}$ single crystals, has initiated wide speculation on the symmetry of the order parameter in HTSC materials.

In this work, I will focus on the fundamentals of the method for measuring impedance and the general properties and features of the $Z_s(T)$ and $\hat{\sigma}(T)$ curves in the normal and superconducting states of different HTSC crystals and discuss the phenomenological model for the description of their microwave response. Emphasis will be on the problems of residual surface resistance, unusually large change $\Delta X_s(T) > \Delta R_s(T)$ in some HTSC crystals, and conductivity anisotropy.

MEASURED QUANTITIES AND SAMPLES

In the centimeter and millimeter wavelength ranges, the surface impedance of small-sized HTSC samples with a surface area of ~1 mm^2 is measured by the so-called hot-finger method. A sample mounted on a sapphire rod was placed in the center of a cylindrical cavity made from Nb and operating at frequency $f = 9.42$ GHz in the H_{011} mode; i.e., the sample was placed in the maximum of a uniform microwave magnetic field $\mathbf{H}_\omega$ [3]. The temperature of the rod and the sample was varied from helium to room temperature without heating of the cavity, which was washed from outside by liquid helium and was always in the superconducting state. At some steady-state temperature T, the microwave power passed through the cavity was recorded as a function of frequency (resonance curve), from which was derived, in the first run, the Q factor $Q_s(T)$ and the frequency

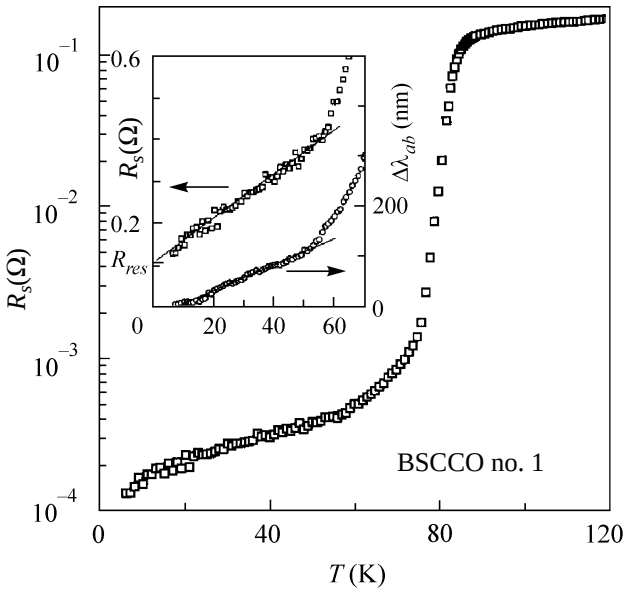

Fig. 1. Surface resistance $R_s(T)$ in the *ab* plane of BSCCO crystal no. 1 at a frequency of 9.4 GHz. Inset: $\Delta\lambda_{ab}(T)$ and $R_s(T)$ dependences at low *T*. The residual surface resistance $R_{res} \approx 120$ μΩ is indicated.

$f_s(T)$ of the cavity with the sample inside and, in the second run, $Q_e(T)$ and $f_e(T)$ of the cavity without the sample. The accuracy of measuring the Q factor ~10^7 was no worse than 1%, and the accuracy of determining the resonance frequency was ~10 Hz. The temperature dependences of the surface resistance R_s and reactance X_s of the sample are found from the relationships

$$R_s(T) = \Gamma_s\Delta(1/Q) = \Gamma_s[Q_s^{-1}(T) - Q_e^{-1}(T)], \quad (1)$$

$$X_s(T) = -2\Gamma_s\frac{\delta f}{f} = -\frac{2\Gamma_s}{f}[\Delta f_s(T) - \Delta f_e(T) - f_0], \quad (2)$$

where Γ_s is the geometric factor of the sample and δf is the frequency difference between the cavity with the sample and the cavity with an ideal conductor, identical in shape and size, into which the magnetic field does not penetrate. The δf value differs from the difference between the measured resonance frequency shifts $\Delta f_s - \Delta f_e = \Delta f$ by a constant f_0, which accounts both for frequency drift caused by the ideal conductor and for irreproducible changes in the cavity reference frequency upon putting in and taking out the sample. It follows from Eqs. (1) and (2) that, to determine the $R_s(T)$ and $X_s(T)$ values from the measured $Q(T)$ and $\Delta f(T)$ values, two quantities need to be known: Γ_s and f_0. The geometric factor Γ_s depends on the shape and size of the crystal and on its orientation about the field $\mathbf{H}_\omega$ in the cavity. The experimental and theoretical methods of determining Γ_s are known [3]; by order of magnitude, it is equal to tens of kiloohms at frequencies ~10 GHz. The f_0 constant can be determined from the measurements of the microwave response in the normal state (see below).

This work will consider the results of measuring the temperature-dependent impedance and conductivity of HTSC copper oxide crystals as platelets with transverse dimensions $a \sim b \sim 1$ mm and thickness $c \sim 0.1$ mm: $YBa_2Cu_3O_{6.95}$ (YBCO, $T_c \approx 93$ K), $Bi_2Sr_2CaCu_2O_{8+\delta}$ (BSCCO no. 1, $T_c \approx 83$ K and BSCCO no. 2, $T_c \approx 92$ K), $Tl_2Ba_2CaCu_2O_{8-\delta}$ (TBCCO, $T_c \approx 112$ K), and $Tl_2Ba_2CuO_{6+\delta}$ (TBCO, $T_c \approx 90$ K). Except for slightly overdoped BSCCO crystal no. 1, whose experimental dependences $R_s(T)$ and $\Delta\lambda_{ab}(T) = \Delta X_s(T)/\omega\mu_0$ in the *ab* plane are shown in Fig. 1, the compositions of all other crystals corresponded to the optimum doping.

Problem 1. The residual surface resistance $R_{res} = R_s(T \longrightarrow 0)$ deserves attention because it determines the quality of a crystal. Whereas the R_{res} value in classical superconductors is clearly defined as a level of the plateau in the $R_s(T)$ curve at $T < T_c/4$, no such plateau occurs in the HTSC crystals, so that by R_{res} is meant the $R_s(T = 0)$ value obtained by extrapolating the linear portion of the $R_s(T)$ curve at $T \ll T_c$ to zero temperature (inset in Fig. 1). It was experimentally established for classical superconductors that $R_{res} \propto \omega^2$ and is determined by various defects in the surface layer of the sample [4, 5]; based on this fact, it is usually agreed that the smaller R_{res} the higher the sample quality. In HTSC materials, the residual resistance also varies quadratically with frequency, but it exceeds the R_{res} value in usual superconductors by a factor of several tens even in the best crystals. When it is considered that the R_{res} value has failed to be noticeably reduced over the last 5–7 years of developing the methods of growing HTSC crystals and, in addition (see below), that the temperature behavior of conductivity $\sigma'(T)$ in the samples of identical chemical composition changes radically with changing R_{res}, then it becomes clear that elucidation of the nature of residual losses in HTSC materials is a highly topical problem.

At $T > 4$ K, the relation between the electric field and the current density in the normal and superconducting states of the HTSC materials has a local character: $j = \hat{\sigma}E$, where $\hat{\sigma}$ is the conductivity tensor which has only two components in a tetragonal crystal, i.e., the conductivity σ_{ab} in the CuO_2 *ab* plane and σ_c across the cuprate planes. In the hot-finger method, the components of the $\hat{\sigma}$ tensor can be found by measuring the microwave response for two crystal orientations about the direction of the $\mathbf{H}_\omega$ field: the transverse (T) $\mathbf{H}_\omega \| \mathbf{c}$ (Fig. 2a) and the longitudinal (L) $\mathbf{H}_\omega \perp \mathbf{c}$ (Fig. 2b) orientations.

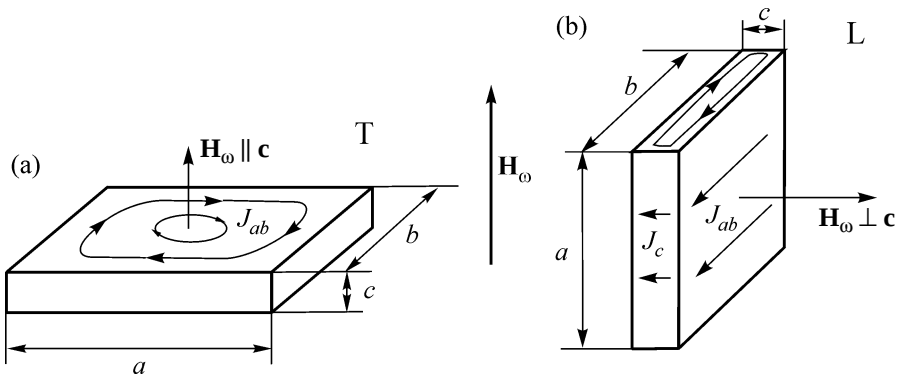

Fig. 2. (a) Transverse (T) crystal orientation, $\mathbf{H}_\omega \parallel \mathbf{c}$. Arrows indicate the direction of high-frequency currents. (b) Longitudinal (L) orientation, $\mathbf{H}_\omega \perp \mathbf{c}$.

ANALYSIS OF EXPERIMENTS WITH TRANSVERSE ORIENTATION

Surface impedance. Let us first consider the T orientation, for which the high-frequency currents circulate in the *ab* plane (Fig. 2a). At frequencies ~10 GHz, the field penetrates into the HTSC sample to a skin depth $\delta_{ab} \sim 5 \times 10^{-3}$ mm at $T \geq T_c$ and to a depth of $\lambda_{ab} \sim 10^{-4}$ mm at $T < T_c$. Since both values are much smaller than the crystal thickness *c*, one can consider the crystal impedance Z_s^{ab} in the T orientation as a coefficient in the Leontovich boundary condition [6] at any temperature and use the local relationship

$$Z_s^{ab} = R_s + iX_s = (i\omega\mu_0/\sigma_{ab})^{1/2} \qquad (3)$$

for the relation between the impedance and the conductivity σ_{ab}. If the microwave conductivity of HTSC is real at $T \geq T_c$, then the f_0 constant [see Eq. (2)] for the T orientation can be found, according to Eq. (3), from the condition that the imaginary and real parts of impedance are equal in the normal state, i.e., by fitting the temperature dependence $R_s(T)$ to $\Delta X_s(T)$ at $T \geq T_c$. This expedient was used to determine the $X_s(T)$ values for BSCCO crystal no. 2 over the entire temperature range (Fig. 3). It should be taken into account that the temperature behavior of the reactance in the T orientation may be noticeably affected by the thermal expansion of the crystal. Since the resonance frequency is determined by the volume occupied by the field, the crystal expansion is equivalent to a decrease in the penetration depth and, thus, leads to an additional frequency shift Δf_t in the square brackets in Eq. (2). It is shown in [3] that, although the contribution of Δf_t to the total frequency shift of the cavity is negligible at low temperatures, it becomes noticeable at $T > 0.9T_c$, especially for the strongly anisotropic HTSC crystals. The $X_s(T)$ dependence in Fig. 3 is constructed with allowance made for the thermal expansion of BSCCO crystal no. 2. Otherwise, i.e., without the Δf_t term in Eq. (2), the reactance curve coincides with the curve in Fig. 3 only up to $T \approx T_c$, while its slope at $T > T_c$ becomes smaller and at $T =$ 150 K the discrepancy is as large as 25 mΩ.

The condition $R_s(T) = X_s(T)$ for the normal skin effect was experimentally proved for the BSCCO [7–9], YBCO [7, 10–12], TBCCO [13], LaSrCuO [14], and BaKBiO [15] crystals at $T \geq T_c$ in the T orientation. All temperature dependences $R_s(T)$ of the HTSC crystals at $T \geq T_c$ fit the formula $2R_s^2(T)/\omega\mu_0 = \rho_{ab}(T) =$

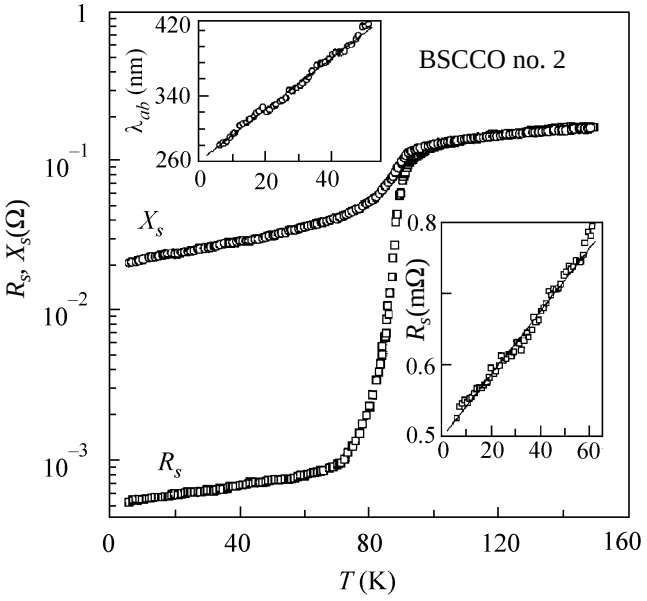

Fig. 3. $R_s(T)$ and $X_s(T)$ for T-oriented BSCCO crystal no. 2 at a frequency of 9.4 GHz. Inset: $\lambda_{ab}(T)$ and $R_s(T)$ dependences at low temperatures.

$\rho_{ab}(0) + bT$ well. For instance, $\rho_{ab}(0) \approx 13$ μΩ cm and $b \approx 0.3$ μΩ cm/K for BSCCO crystal no. 2.

Problem 2. The behavior of $Z_s(T)$ for the TBCO [16, 17] and HgBaCuO crystals is also under debate.[1] Even if one achieves coincidence between the $R_s(T)$ and $\Delta X_s(T)$ curves at $T \geq T_c$, i.e., $R_s(T) = X_s(T)$, the variation $\Delta X_s(T)$ of the reactance in the superconducting state $T < T_c$ proves to be so much larger than $\Delta R_s(T)$ that $X_s(0)$ becomes negative. In addition, the problem is complicated by the lack of literature data for the thermal expansion coefficients of the TBCO and HgBaCuO crystals. If one assumes that at $T > T_c$ the corresponding coefficient for the cuprate planes of TBCO is the same as in the BSCCO [18] or TBCCO [19] crystal and takes account of the $\Delta f_t(T)$ shift in Eq. (2), then the $R_s(T)$ and $X_s(T)$ curves in the normal state of TBCO become mutually parallel. However, an attempt at achieving coincidence through satisfying the condition for the normal skin effect leads to the $X_s(0) = \omega\mu_0\lambda_{ab}(0) < 0$ value. Therefore, the problem amounts to revealing either the cause for the appearance of a negative increment $dX_s < 0$ at $T < T_c$ that must be subtracted from the measured $\Delta X_s(T)$ curve in order to obtain the true value $X_s(T) > 0$ for the reactance coinciding with $R_s(T)$ at $T > T_c$ or the cause explaining the positive difference $X_s(T) - R_s(T)$ in the normal state of TBCO and providing a reasonable value $X_s(0) > 0$. In this respect, the following two growth and structural features of the TBCO crystals distinguish them from BSCCO. It is known that the so-called cleavage planes may crop out at the surface of the TBCO crystal, whereas the surface of the BSCCO crystal is smooth. If the traces of these planes form ridges (valleys) in the form of extended channels at the surface and if the sizes (height, width, spacing) of these roughnesses exceed the penetration depth for the field normal to the surface, then, as shown in [5], field screening by such roughnesses gives rise to a negative addition $dX_s < 0$ to the measured reactance $X_s(T)$. With a rise in temperature, the penetration depth increases and, at a certain $T^* < T_c$, reaches the roughness size. For this reason, the addition dX_s to the reactance can be ignored at $T > T^*$. Another possible reason why the measured $X_s(T)$ value is larger than $R_s(T)$ in the normal state of TBCO is the size effect in the T orientation. The unit cell of BSCCO contains two conducting CuO_2 planes, while the unit cell of TBCO, though being of approximately the same size, contains only one such plane. If the high-frequency currents mainly decay in these planes, then the screening thickness c^* of the TBCO crystal will be less than its actual thickness c and might be comparable with the skin depth. One can expect from the solution of the electrodynamic problem of field distribution in a T-oriented thin plate that, owing to the size effect, the measured effective $X_s^{\text{eff}}(T)$ value is greater than the effective $R_s^{\text{eff}}(T)$ at $T \geq T_c$.

The conductivity σ_{ab} in the superconducting state is a complex value, and, according to Eq. (3), the real R_s and imaginary X_s parts of the impedance are not equal to each other:

$$R_s(T) = \sqrt{\frac{\omega\mu_0(\varphi^{1/2} - 1)}{2\sigma''\varphi}},$$
$$X_s(T) = \sqrt{\frac{\omega\mu_0(\varphi^{1/2} + 1)}{2\sigma''\varphi}}, \quad (4)$$

where $\varphi = 1 + (\sigma'/\sigma'')^2$. Evidently, $R_s(T) < X_s(T)$ at $T < T_c$. For $\sigma' \ll \sigma''$, which is the case in the temperature range not too close to T_c, one has from Eq. (4)

$$R_s \simeq \frac{(\omega\mu_0)^{1/2}\sigma'}{2(\sigma'')^{3/2}} = \frac{1}{2}\omega^2\mu_0^2\sigma'\lambda^3,$$
$$X_s \simeq \left(\frac{\omega\mu_0}{\sigma''}\right)^{1/2} = \omega\mu_0\lambda. \quad (5)$$

The linear dependence of the reactance $\Delta X_s(T) \propto \Delta\lambda_{ab}(T) \propto T$ and the linear dependence of the surface resistance $\Delta R_s(T) \propto T$ at frequencies ~10 GHz and below are the regularities common to all HTSC crystals at $T \ll T_c$ (see Figs. 1, 3 and reviews [3, 20–22] and references therein). The slopes of the $\Delta\lambda_{ab}(T)$ straight lines at $T \ll T_c$ are different. For example, in the YBCO crystals prepared by different methods, the slopes for $\Delta\lambda_{ab}(T)$ may diverge by approximately an order of magnitude [12, 23, 24]. The $Z_s(T)$ curves for the BSCCO, TBCCO, and TBCO crystals with tetragonal lattice also differ from those for the orthorhombic YBCO crystals. Whereas the linear dependence $\Delta R_s(T) \propto T$ at frequencies ~10 GHz for the first of them may extend up to $T_c/2$ (Figs. 1, 3), in YBCO it terminates at $T < T_c/3$ and gives way to a broad peak in $R_s(T)$ (Fig. 4). With an increase in frequency, the peak shifts to higher temperatures and its amplitude decreases. It is also known that the higher the quality of the YBCO crystal the larger the peak amplitude and the lower the temperature of its occurrence [25]. Finally, the $\lambda_{ab}(T)$ [12, 23] and $R_s(T)$ [23] curves for single crystal YBCO show some features in the intermediate temperature range $T \sim T_c/2$.

Complex conductivity. The $\sigma'(T)$ and $\sigma''(T)$ components are not determined directly from the experiment but can be found from Eq. (4) after measuring, according to Eqs. (1) and (2), the $R_s(T)$ and $X_s(T)$ values:

$$\sigma' = \frac{2\omega\mu_0 R_s X_s}{(R_s^2 + X_s^2)^2}, \quad \sigma'' = \frac{\omega\mu_0(X_s^2 - R_s^2)}{(R_s^2 + X_s^2)^2}. \quad (6)$$

[1] S. Sridhar, private communication.

It should be emphasized that, to determine the conductivity components, it is necessary to know the $R_s(T)$ and $X_s(T)$ values in absolute units. At temperatures not too close to T_c, $R_s(T) \ll X_s(T)$ for the HTSC crystals. Consequently, the $\sigma''(T)$ curves are determined solely by the $X_s(T) = \omega\mu_0\lambda(T)$ function and reflect the main features of the temperature behavior of the penetration depth, namely, its linear temperature dependence at low temperatures for all high-quality HTSC crystals and the features observed for YBCO in the intermediate temperature range. The shape of the $\sigma'_{ab}(T)$ curve depends on the residual surface resistance R_{res}. It follows from Eq. (6) that $\sigma'_{ab}(T)$ has a maximum at $T < T_c$ if [22]

$$R_{res} < \frac{X_s(0)}{3}\frac{dR_s(T)}{dX_s(T)}\bigg|_{T\to 0}. \qquad (7)$$

As R_{res} increases, the peak in the $\sigma'_{ab}(T)$ curve shifts to lower temperatures and disappears when R_{res} reaches the value equal to the right-hand side of Eq. (7). If the R_{res} value for the crystal is such that inequality (7) breaks, the conductivity $\sigma'_{ab}(T)$ becomes a monotonically decreasing function of temperature at $T < T_c$. Figure 5 demonstrates both possible shapes of the $\sigma'_{ab}(T)$ curves at a frequency of 9.4 GHz, namely, the peak for BSCCO crystal no. 1 (Fig. 5a, $R_{res} \approx 120$ μΩ) and its absence for BSCCO crystal no. 2 (Fig. 5b, $R_{res} \approx$ 500 μΩ). The higher the crystal quality, the more pronounced the conductivity peak at $T < T_c$. The $\sigma'_{ab}(T)$ curve in Fig. 6 corresponds to the $R_s(T)$ dependence obtained for the YBCO crystal at a frequency of 1.14 GHz (Fig. 4, $R_{res} \sim 1$ μΩ). Beginning with a steep linear portion, the $\sigma'_{ab}(T)$ curve rapidly reaches its maximum value, which always markedly exceeds the conductivity $\sigma'(T_c)$ in the normal state. As the frequency increases, the peak in $\sigma'_{ab}(T)$ shifts to higher temperatures and its amplitude decreases. At temperatures close to T_c, the $\sigma'(T)$ curve for the HTSC materials is shaped like a narrow peak with width virtually coinciding with the width of the superconducting transition in the $R_s(T)$ curve.

Modified two-fluid model (MTM). A simple way of describing all the observed $Z_s^{ab}(T)$ and $\sigma_{ab}(T)$ dependences was suggested in [15, 26] and further developed in [3, 21, 22, 27, 28]. The idea consists in the extension of a Gorter–Casimir (GC) two-fluid model [29] to the HTSC materials, which are characterized by high T_c values. In metals, the quasiparticle inelastic scattering at such temperatures becomes essential and, hence, the GC model should be naturally modified by incorporating the temperature-dependent relaxation time τ for the quasiparticles of a "normal fluid." Assuming that the scattering processes in this fluid are

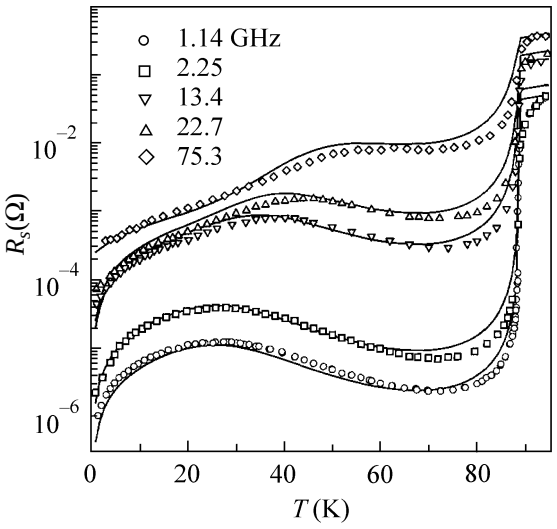

Fig. 4. Symbols correspond to the $R_s(T)$ values measured in the *ab* plane of YBCO crystal at different frequencies [25]. Solid lines correspond to the calculations by Eqs. (4), (8), and (9) with $\kappa = 9$ and experimentally determined $\tau(T_c) = 10^{-13}$ s, $\beta = 0.005$, and $n_s(T)/n = \sigma''(T)/\sigma''(0)$. To the $R_s(T)$ value calculated for the upper curve (75.3 GHz) $R_{res} = 0.3$ mΩ was added.

similar to those occurring in normal metals, we used the Bloch–Grüneisen formula (electron–phonon scattering) for the function $\tau(T)$ in the normal and superconducting states of HTSC and retained the temperature-independent impurity relaxation time $\tau(0)$, which is present in the standard GC model:

$$\frac{1}{\tau} = \frac{1}{\tau(0)}\left[1 + \frac{t^5 \mathcal{J}_5(\kappa/t)/\mathcal{J}_5(\kappa)}{\beta}\right],$$
$$\mathcal{J}_5(\kappa/t) = \int_0^{\kappa/t} \frac{z^5 e^z dz}{(e^z - 1)^2}, \qquad (8)$$

where $t \equiv T/T_c$; $\kappa = \Theta/T_c$ (Θ is the Debye temperature); and β is a numerical parameter equal, according to Eq. (8), to $\tau(T_c)/[\tau(0) - \tau(T_c)]$. Following the formal analogy to metals, one can state that β characterizes the "degree of purity" of HTSC material: $\beta \approx \tau(T_c)/\tau(0) \ll 1$ if $\tau(0) \gg \tau(T_c)$. It is shown in [22] that the parameter β can be derived from the measured $R_s(T)$ and $X_s(0)$ values and the dR_s/dT and dX_s/dT slopes at $T \ll T_c$. The Θ temperature for HTSC is estimated at several hundred degrees. At $T < \Theta/10$ ($\kappa > 10t$), the second term in the square brackets in Eq. (8) is proportional to T^5 and at $T > \Theta/5$ ($\kappa < 5t$), it is proportional to T. Therefore, at $\beta < 1$, the inverse relaxation time (coefficient of quasiparticle decay) equals $1/\tau(0)$ in the range $T \ll T_c$ and monotonically increases with temperature following a power law from $\propto T^5$ to $\propto T$ near T_c, thereby providing the linear temperature dependence $\Delta\rho_{ab}(T) \propto 1/\tau(T) \propto T$ at $T > T_c$.

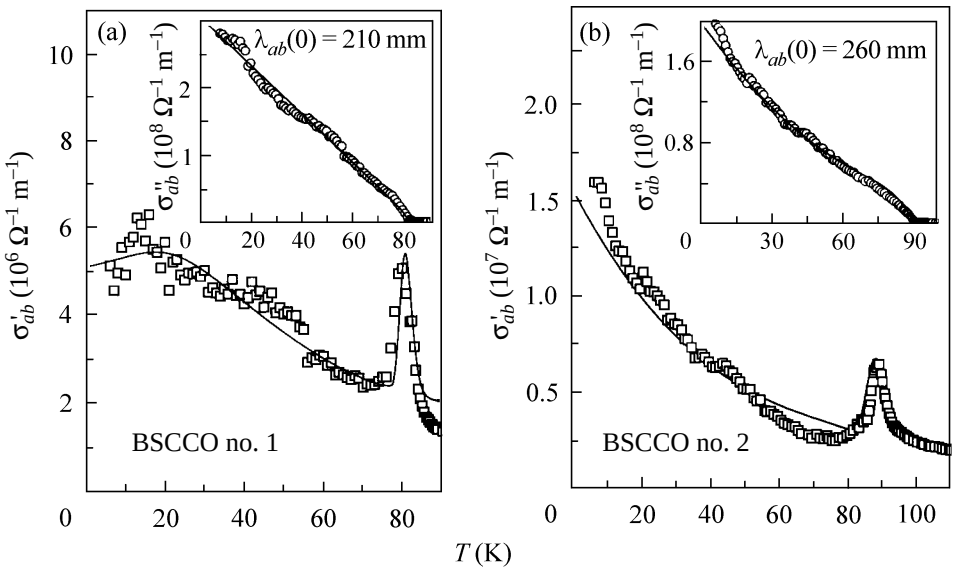

Fig. 5. Symbols correspond to $\sigma'_{ab}(T)$ and (inset) $\sigma''_{ab}(T)$ determined for BSCCO crystal nos. 1 and 2 by Eq. (6) using the measured $R_s(T)$ and $X_s(T)$ values. Solid lines correspond to the calculations by Eqs. (8) and (9) with $\kappa = 2$ for BSCCO crystal no. 1 and $\kappa = 3$ for no. 2 and experimental values $T_c = 83$ K, $\delta T_c = 2.5$ K, $\omega\tau(T_c) = 7 \times 10^{-3}$, $\beta = 0.3$, $\alpha = 1$, and $R_{res} = 120$ μΩ for BSCCO no. 1 and $T_c = 92$ K, $\delta T_c = 4.5$ K, $\omega\tau(T_c) = 9 \times 10^{-3}$, $\beta = 2$, $\alpha = 2$, and $R_{res} = 500$ μΩ for BSCCO no. 2.

Despite the fairly simplified form of $\tau(T)$ chosen for HTSC materials with a complex band structure, it turns out that all common and specific features of the $R_s(T)$ and $\sigma'_{ab}(T)$ curves are adequately described by the MTM with only one fitting parameter κ in Eq. (8). Indeed, the conductivity components are

$$\sigma' = \frac{n_n e^2 \tau}{m} \frac{1}{1 + (\omega\tau)^2},$$
$$\sigma'' = \frac{n_s e^2}{m\omega}\left[1 + \frac{n_n}{n_s}\frac{(\omega\tau)^2}{1 + (\omega\tau)^2}\right], \quad (9)$$

where $n_n(T)$ and $n_s(T)$ are the densities of the normal and superconducting carriers, respectively (both have the same charge e and mass m); the total concentration $n = n_n + n_s$ is equal to the concentration of charge carriers in the normal state and is independent of T. Making use of the measured dependence $n_s(T)/n = \sigma''(T)/\sigma''(0) = \lambda^2(0)/\lambda^2(T)$ and, hence, determining the function $n_n(T)/n = 1 - n_s(T)/n$, one can chose the κ parameter for the sample of interest using Eqs. (8) and (9) to describe, first by Eq. (4), all the above-mentioned experimental $R_s(T)$ curves and, next by Eq. (6), the real part $\sigma'_{ab}(T)$ of the conductivity for the T-oriented HTSC crystal. The solid lines in Figs. 4–6 are examples of a comparison between the experimental and MTM curves.

Here, I should enlarge upon two important points that have not yet been discussed but were implicitly used in the calculations. First, account was taken of the inhomogeneous broadening δT_c of superconducting transition near T_c. This was done using the approach that was suggested in [21, 22] and gave rise to a maximum of the effective conductivity $\sigma'(T)$ at temperature $T_m = T_c - \delta T_c$ close to the critical temperature. The relative amplitude of this peak $[\sigma'(T_m) - \sigma(T_c)]/\sigma(T_c)$ is inversely proportional to the frequency and decreases with decreasing width (δT_c) of the superconducting transition [22].

Second, when comparing with the experimentally measured surface resistance, the temperature-independent R_{res} value was taken from the same experiment and added to the $R_s(T)$ value calculated using general Eq. (4). That is why the $\sigma'_{ab}(T)$ curves calculated by Eq. (6) do not turn to zero at $T \longrightarrow 0$ in Fig. 5, although the two-fluid model assumes that the density $n_n = 0$ at $T = 0$ and, according to Eq. (9), the conductivity $\sigma'(0) = 0$. The R_{res} value was not taken into account when comparing with the data in Figs. 4 (except for the upper curve) and 6 because the corresponding $R_{res}/R_s(T)$ ratios are very small (less than 10^{-3}). In most HTSC crystals, $R_{res}/R_s(T_c) > 10^{-3}$, so that the effect of the residual surface resistance becomes noticeable at $T \ll T_c$. One more reason for the inclusion of R_{res} is that the ratio $R_{res}/R_s(T_c) \propto \omega^{3/2}$ increases with frequency and becomes appreciable for the upper curve in Fig. 4.

Problem 1 (continued). The question of the nature of the residual losses remains open for HTSC materials. In some works (see, e.g., [30]), the origin of these losses was explained by the presence of a certain

amount n_0 of unpaired carriers in the sample at $T = 0$. The R_{res} value was estimated by using Eq. (5) with nonzero conductivity $\sigma'(0) = n_0 e^2 \tau(0)/m$ [Eq. (9) at $(\omega\tau)^2 \ll 1$]. However, it can easily be shown that the R_{res} values thus determined must satisfy inequality (7); otherwise, as it may occur for the HTSC crystals (see Fig. 5b), the n_0 value would exceed the total carrier concentration n. In many works developing the traditional approach assigning the residual resistance to various surface imperfections, the losses were explained by the presence of weak links [31–33], twin boundaries [33, 34], normally conducting clusters [35], etc. However, estimates show that the contribution from such losses is small compared to the R_{res} values measured in the HTSC materials. In addition, the residual surface resistance is approximately the same in perfect HTSC copper oxide crystals prepared by different methods or having different chemical compositions, containing twins or not, and with a freshly cleaved surface or as-grown surface: $R_{res} \sim 100$ μΩ at a frequency of 10 GHz. This fact indicates that the origin of residual losses has an "intrinsic" character and is inherent in all high-quality HTSC crystals. It is most likely associated with the structural features of these materials, namely, with the pronounced layered structure of these compounds. In other words, the current in the surface layer of HTSC crystals may flow in a nonsuperconducting part of the layer possessing a finite resistivity ρ_n. In the model under discussion, this additional contribution can be taken into account as a circuit element ρ connected in parallel to the two-fluid circuit characterized by Eq. (9), i.e., as a resistance $\rho = 1/\sigma'$ shunted by a kinetic inductance $l = 1/\omega\sigma''$ (parallel connection of ρ and l corresponds to the coupling adopted between current and field in the two-fluid model). Evidently, the complex circuit impedance consists of the imaginary part $iX_s = i\omega\mu_0\lambda$ at $T < T_c$ and the sum of two real terms: R_s from Eq. (5) and $R_0 = \omega^2\mu_0^2\lambda^3/2\rho_n$. At $T = 0$, when $R_s(0) = 0$, the latter can play the role of a residual surface resistance R_{res} proportional to ω^2, as it follows from the experiments. At a frequency of 10 GHz and for the $R_{res} \approx 100$ μΩ and $\lambda(0) \approx 0.2$ μm values typical of HTSC crystals, one obtains a typical metallic value $\rho_n(0) \approx 25$ μΩ cm. According to the above-mentioned procedure of comparison with the experimental $R_s(T)$ curves, one must also require that R_0 be independent of temperature at $T \ll T_c$. This is possible if $\rho_n(T) \propto \lambda^3(T)$; i.e., $\rho_n(T)$ should vary linearly with temperature at $T \ll T_c$: $\rho_n(t) = \rho_n(0)(1 + 1.5\alpha t)$, where α is the slope of the $\sigma''(t)$ curve at $t \ll 1$ in this sample:

$$\sigma''(t)/\sigma''(0) = \lambda^2(0)/\lambda^2(t) \simeq (1 - \alpha t). \qquad (10)$$

The coefficients $\rho_n(0)$ and $1.5\alpha\rho_n(0)/T_c$ in BSCCO crystal no. 2 are approximately equal to the coefficients $\rho_{ab}(0)$ and b in the expression $\rho_{ab}(T) = \rho_{ab}(0) + bT$ for the resistivity of this sample in the normal state; i.e., $\rho_n(T) \approx 2R^2(T)/\omega\mu_0$, where $R(T)$ is the continuation of the $R_s(T)$ line at $T > T_c$ (Fig. 3) to the superconducting region $T < T_c$ (down to $T = 0$).

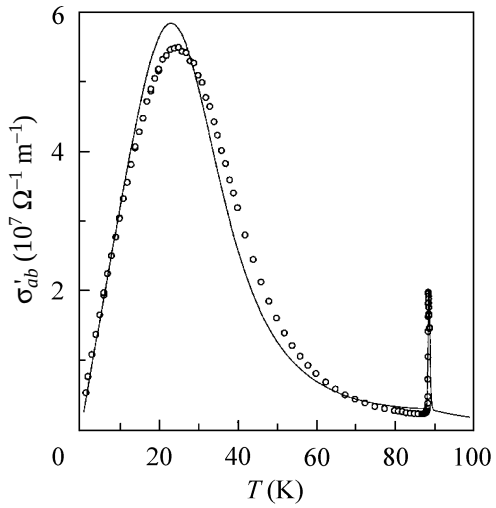

Fig. 6. (Circles) $\sigma'_{ab}(T)$ for YBCO crystal at a frequency of 1.14 GHz [25] and (solid line) the calculation by Eqs. (8) and (9) with $\kappa = 9$, $\tau(T_c) = 10^{-13}$ s, $\beta = 0.005$, and $\delta T_c = 0.4$ K.

It would be appropriate to close the discussion of the MTM by writing formulas describing the experimental data $n_s(T)/n = \sigma''(T)/\sigma''(0)$, which were used for calculating $R_s(T)$ and $\sigma'_{ab}(T)$ in the T orientation. There are several variants of such empirical formulas [3, 21, 22, 26, 27]. All of them have the form of Eq. (10) at $T \ll T_c$, because all $\sigma''_{ab}(T)$ curves for HTSC single crystals are characterized by the linear dependence at low temperatures.

Thus, the model based on Eqs. (8)–(10) adequately describes the general properties of the $Z_s(T)$ and $\sigma_{ab}(T)$ curves for high-quality HTSC crystals. It follows from these formulas that all curves have a linear portion at $t \ll 1$: $\sigma' \propto \alpha t/\beta$, because $n_n/n \approx \alpha t$ and $\tau \approx \tau(0) \approx \tau(T_c)/\beta$; $\Delta\sigma'' \propto -\alpha t$; $R_s \propto \alpha t/\beta$ according to Eq. (5); and $\Delta X_s \propto \Delta\lambda \propto \alpha t/2$. As the temperature increases, the $\sigma'(t)$ function passes through a maximum at $t < 0.5$ if the residual surface resistance R_{res} is so small that inequality (7) is fulfilled. This peak arises from the superposition of two opposite effects: a decrease in the number of normal carriers with decreasing temperature at $t < 1$ and an increase (terminating at $t \sim \beta^{1/5}$) in the relaxation time. If Eq. (7) is not fulfilled, $\sigma'(t)$ monotonically decreases with temperature elevation. This model also describes the temperature dependences of the surface impedance and the complex conductivity of YBCO single crystals grown by different methods. The postulates and consequences of the MTM are analyzed in recent works [21, 22] from the viewpoint of modern microscopic theories of the microwave response of HTSC materials.

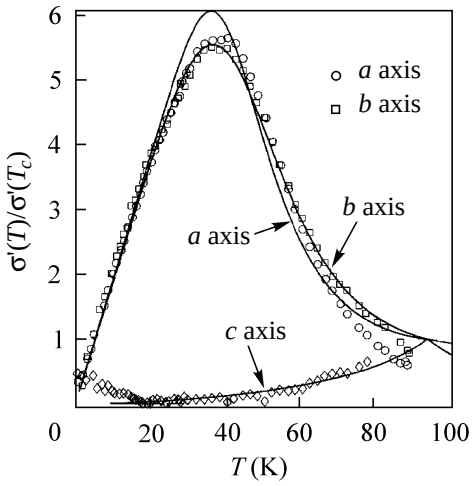

Fig. 7. (Symbols) components of the conductivity tensor $\hat{\sigma}'(T)/\hat{\sigma}(T_c)$ for YBCO at a frequency of 22 GHz [40] at $T < T_c$. (Solid lines) calculations [28] by Eqs. (8) and (9).

CONDUCTIVITY OF HTSC CRYSTALS ALONG THE *c* AXIS

Problem 3. Let us now consider the L orientation of a crystal with respect to the $\mathbf{H}_\omega$ field in the cavity, $\mathbf{H}_\omega \perp \mathbf{c}$ (Fig. 2b). In the superconducting state, the high-frequency currents flowing in the *ab* planes decay at a depth of λ_{ab}, while the *c*-directed currents decay at a depth of λ_c. At $T < 0.9T_c$, these values are small compared to the characteristic sizes of the crystal, allowing one to introduce the effective impedance Z_s^{ab+c} for the L orientation, defined as a surface-averaged value $Z_s^{ab+c} \simeq (bZ_s^{ab} + cZ_s^c)/(b + c)$, where the superscripts on Z_s indicate the directions of screening currents. By measuring $Z_s^{ab}(T)$ in the T orientation and Z_s^{ab+c} in the L orientation, one can determine the losses $R_s^c(T)$ and a change $\Delta\lambda_c(T) = \Delta X_s^c(T)/\omega\mu_0$ [8, 10, 14, 36–39]. To determine $\lambda_c(T)$, one is forced to invoke the results of independent measurements of $\lambda_c(0)$. The literature data on the low-temperature behavior of $\Delta\lambda_c(T)$ are controversial. Both linear dependence $\Delta\lambda_c(T) \propto T$ at $T < T_c/3$ [36, 39] and quadratic dependence [40] were observed even for the most extensively studied YBCO single crystals. In BSCCO crystals, the behavior of $\Delta\lambda_c(T)$ depends on the level of doping with oxygen: in the crystals with maximal $T_c \simeq 90$ K the linear dependence $\Delta\lambda_c(T)$ [8, 9, 38] converts into quadratic [38] as the oxygen content increases.

In recent work [40], detailed measurements of the impedance anisotropy were carried out and the conductivity components along the crystallographic axes were found for the optimum-doped untwinned YBCO crystals. In [28], we undertook an attempt at applying the MTM to the totality of experimental data obtained in [40]. For the real parts of the conductivity tensor, the comparison is shown in Fig. 7 [28]. The peak in $\sigma_c'(T)$ is absent because the temperature dependence of the relaxation time of normal quasiparticles along the *c* axis is very weak at $T < T_c$; i.e., $\tau_c(T) \approx$ const and $\beta_c \gg 1$ in Eq. (8). Moreover, since the inductive losses due to the large λ_c value markedly exceed the active losses (small R_s^c and σ_c' values), it is likely that the microwave *c*-response is mainly caused by the tunneling of Cooper pairs between the CuO_2 planes. Note that, according to the measurements in [40], the surface resistance $R_s^c(T) < R_s^{ab}(T)$ in the range $10 < T < 65$ K. However, in all previous works, the loss measurements

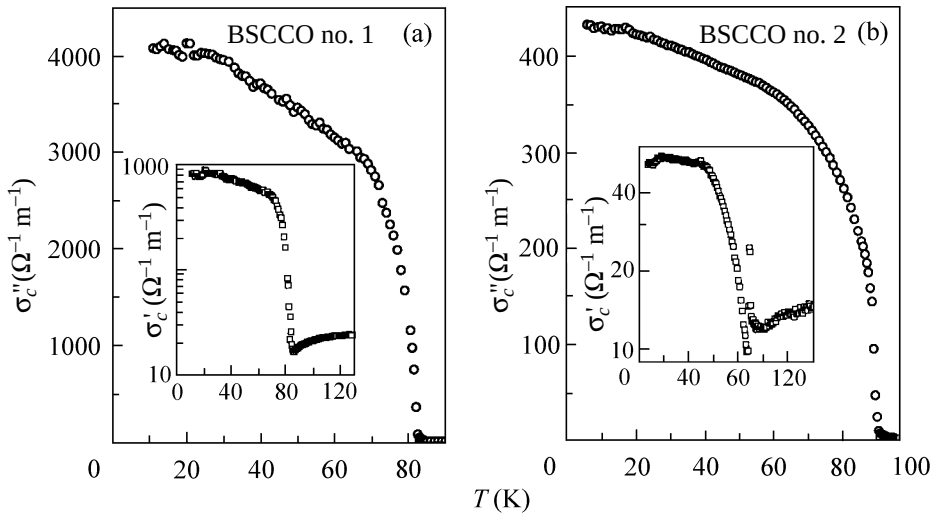

Fig. 8. Conductivity components $\sigma_c''(T)$ and $\sigma_c'(T)$ for BSCCO crystal nos. 1 and 2.

for the optimum-doped HTSC crystals gave the reverse relation $R_s^c(T) \gg R_s^{ab}(T)$ at $T < T_c$.

The aforementioned approach to studying the impedance anisotropy for HTSC crystals at $T < T_c$ gives no way of determining the $\lambda_c(T)$ value from the measurements of the Q factor and the resonance frequency shift in the L orientation and, in addition, cannot be extended to higher temperatures. The point is that the size effect becomes significant at $T > 0.9T_c$ in the L orientation and is the cause of the divergence between the temperature behavior of the effective $R_{s,\,\mathrm{eff}}^{ab+c}(T)$ value measured in the normal state and the $\Delta X_{s,\,\mathrm{eff}}^{ab+c}(T)$ value; as a result, the f_0 constant in Eq. (2) cannot be determined, as it was done previously. Recently [9], we suggested a new procedure for the determination of the f_0 value in the L orientation and, hence, the conductivity components $\sigma_c'(T)$ and $\sigma_c''(T)$ along the c axis. The procedure is based on the known formulas [41] allowing for the size effect in the field distribution in a long anisotropic strip with size $a \gg b, c$ (Fig. 2b). The $\sigma_c'(T)$ and $\sigma_c''(T)$ dependences obtained for BSCCO crystal nos. 1 and 2 using this procedure are shown in Fig. 8 [42]. The $\lambda_c(0)$ value proved to be equal to approximately 50 μm for sample no. 1 and 150 μm for sample no. 2, in agreement with the results of our measurements of $\lambda_c(0)$ in these crystals by other methods [43, 44]. One can see from Fig. 8 that the conductivity $\sigma_c'(T)$ in both samples grows with decreasing temperature at $T < T_c$, despite the fact that the $\sigma_{ab}'(T)$ dependences in these crystals are different (Fig. 5). The formal reason for this growth is clear: the residual losses R_{res}^c along the c axis of BSCCO crystal nos. 1 and 2 are large enough so that inequality (7) breaks. At the same time, the $\sigma_c'(T)$ dependences measured for BSCCO crystals by other techniques [45, 46] showed semiconductor behavior at $T < T_c$.

CONCLUSION

The results of measuring the surface impedance and the complex conductivity of the T-oriented ($\mathbf{H}_\omega \parallel \mathbf{c}$) optimum-doped samples of different chemical composition are systematized and described within the framework of the MTM. The common feature of the experimental $Z_s^{ab}(T)$ and $\sigma_{ab}(T)$ curves obtained for HTSC single crystals is that the conductivity components $\sigma_{ab}'(T)$ and $\sigma_{ab}''(T)$, the reactance $\Delta X_s(T) \propto \Delta\lambda_{ab}(T) \propto T$, and the surface resistance $\Delta R_s(T) \propto T$ linearly depend on temperature at $T \ll T_c$. In terms of the MTM, such behavior of the microwave response of HTSC materials is caused by the linear decrease in the density $n_s(T)$ of superconducting carriers with a rise in temperature at $T \ll T_c$. A broad peak at $T < T_c$ in the $R_s^{ab}(T)$ curve is the distinctive feature of the YBCO crystals. In the MTM, the presence or absence of this peak is governed by a change in $\tau(T)$ in the temperature range $0 < T < T_c$: whereas the $\tau(T_c) \approx 10^{-13}$ s value is approximately the same for all high-quality HTSC crystals at $T = T_c$, the $\tau(0)$ value in YBCO is greater than $\tau(0)$ in other compounds by a factor of ten and more at $T \ll T_c$. The reason why the change in the reactance $\Delta X_s(T)$ exceeds the change in the surface resistance $\Delta R_s(T)$ of TBCO crystals remains to be clarified. The origin of residual losses in HTSC is among the hottest problems because the behavior of real components $\hat{\sigma}'(T)$ of the conductivity tensor is governed at $T < T_c$ by this quantity. The anisotropy of high-frequency conductivity of HTSC materials also calls for detailed study.

I am grateful to all participants (I.E. Batov, A.A. Zhukov, G.V. Merzlyakov, Yu.A. Nefedov, A.T. Sokolov, G.É. Tsydynzhapov, A.F. Shevchun, and D.V. Shovkun) of project nos. 97-02-16836 and 00-02-17053 of the Russian Foundation for Basic Research for collaboration and activity. Discussions with V.F. Gantmakher, A.A. Golubov, and E.G. Maksimov were very useful. I appreciate fruitful collaboration with foreign colleagues A. Agliolo-Gallitto, N. Bontemps, A. Buzdin, I. Ciccarello, H. Fink, J. Halbritter, M. Li Vigni, S. Sridhar, and T. Tamegai and the support of the CNRS-RAS (grant no. 4985), CLG NATO, Coll. Int. Li Vigni, and RFFI-NNIO (project no. 00-02-04021).

REFERENCES

1. J. Bardeen, L. N. Cooper, and J. R. Schrieffer, Phys. Rev. **108**, 1175 (1957).
2. W. N. Hardy, D. A. Bonn, D. C. Morgan, *et al.*, Phys. Rev. Lett. **70**, 3999 (1993).
3. M. R. Trunin, Usp. Fiz. Nauk **168**, 931 (1998) [Phys. Usp. **41**, 843 (1998)]; J. Supercond. **11**, 381 (1998).
4. J. P. Turneaure, J. Halbritter, and H. A. Schwettman, J. Supercond. **4**, 341 (1991).
5. F. F. Mende and A. A. Spitsyn, *Surface Impedance of Superconductors* (Naukova Dumka, Kiev, 1985).
6. L. D. Landau and E. M. Lifshitz, *Course of Theoretical Physics*, Vol. 8: *Electrodynamics of Continuous Media* (Fizmatlit, Moscow, 1982; Pergamon, New York, 1984).
7. T. Shibauchi, A. Maeda, H. Kitano, *et al.*, Physica C (Amsterdam) **203**, 315 (1992).
8. T. Jacobs, S. Sridhar, Q. Li, *et al.*, Phys. Rev. Lett. **75**, 4516 (1995).
9. D. V. Shovkun, M. R. Trunin, A. A. Zhukov, *et al.*, Pis'ma Zh. Éksp. Teor. Fiz. **71**, 132 (2000) [JETP Lett. **71**, 92 (2000)].
10. H. Kitano, T. Shibauchi, K. Uchinokura, *et al.*, Phys. Rev. B **51**, 1401 (1995).
11. D. Achir, M. Poirier, D. A. Bonn, *et al.*, Phys. Rev. B **48**, 13184 (1993).

12. M. R. Trunin, A. A. Zhukov, G. A. Emel'chenko, *et al.*, Pis'ma Zh. Éksp. Teor. Fiz. **65**, 893 (1997) [JETP Lett. **65**, 938 (1997)].
13. A. A. Zhukov, M. R. Trunin, A. T. Sokolov, *et al.*, Zh. Éksp. Teor. Fiz. **112**, 2210 (1997) [JETP **85**, 1211 (1997)].
14. T. Shibauchi, H. Kitano, K. Uchinokura, *et al.*, Phys. Rev. Lett. **72**, 2263 (1994).
15. M. R. Trunin, A. A. Zhukov, G. É. Tsydynzhapov, *et al.*, Pis'ma Zh. Éksp. Teor. Fiz. **64**, 783 (1996) [JETP Lett. **64**, 832 (1996)].
16. J. R. Waldram, D. M. Broun, D. C. Morgan, *et al.*, Phys. Rev. B **59**, 1528 (1999).
17. N. Hakim, Yu. A. Nefyodov, S. Sridhar, *et al.*, unpublished.
18. C. Meingast, A. Junod, and E. Walker, Physica C (Amsterdam) **272**, 106 (1996).
19. M. Hasegawa, Y. Matsushita, and H. Takei, Physica C (Amsterdam) **267**, 31 (1996).
20. D. A. Bonn and W. N. Hardy, in *Physical Properties of High Temperature Superconductors V*, Ed. by D. M. Ginsberg (World Scientific, Singapore, 1995), p. 7.
21. M. R. Trunin and A. A. Golubov, in *HTSC Spectroscopy*, Ed. by N. M. Plakida (Gordon and Breach, London, 2001) (in press).
22. M. R. Trunin, Yu. A. Nefyodov, and H. J. Fink, Zh. Éksp. Teor. Fiz. **118**, 923 (2000) [JETP **91**, 801 (2000)].
23. H. Srikanth, B. A. Willemsen, T. Jacobs, *et al.*, Phys. Rev. B **55**, R14733 (1997).
24. S. Kamal, R. Liang, A. Hosseini, *et al.*, Phys. Rev. B **58**, R8933 (1998).
25. A. Hosseini, R. Harris, S. Kamal, *et al.*, Phys. Rev. B **60**, 1349 (1999).
26. H. J. Fink, Phys. Rev. B **58**, 9415 (1998).
27. H. J. Fink and M. R. Trunin, Physica B (Amsterdam) **284**, 923 (2000); H. J. Fink, Phys. Rev. B **61**, 6346 (2000).
28. H. J. Fink and M. R. Trunin, Phys. Rev. B **62**, 3046 (2000).
29. C. S. Gorter and H. Casimir, Phys. Z. **35**, 963 (1934).
30. M. Hein, T. Kaiser, and G. Müller, Phys. Rev. B **61**, 640 (2000).
31. T. L. Hylton and M. R. Beasly, Phys. Rev. B **39**, 9042 (1989).
32. A. M. Portis and D. W. Cooke, Supercond. Sci. Technol. **5**, S395 (1992).
33. J. Halbritter, J. Appl. Phys. **68**, 6315 (1990); **71**, 339 (1992).
34. O. G. Vendik, A. B. Kozyrev, and A. Yu. Popov, Rev. Phys. Appl. **25**, 255 (1990).
35. O. G. Vendik, L. Kovalevich, A. P. Mitrofanov, *et al.*, Sverkhprovodimost: Fiz., Khim., Tekh. **3**, 1573 (1990).
36. J. Mao, D. H. Wu, J. L. Peng, *et al.*, Phys. Rev. B **51**, 3316 (1995).
37. D. A. Bonn, S. Kamal, K. Zhang, *et al.*, J. Phys. Chem. Solids **56**, 1941 (1995).
38. T. Shibauchi, N. Katase, T. Tamegai, *et al.*, Physica C (Amsterdam) **264**, 227 (1996).
39. H. Srikanth, Z. Zhai, S. Sridhar, *et al.*, J. Phys. Chem. Solids **59**, 2105 (1998).
40. A. Hosseini, S. Kamal, D. A. Bonn, *et al.*, Phys. Rev. Lett. **81**, 1298 (1998).
41. C. E. Gough and N. J. Exon, Phys. Rev. B **50**, 488 (1994).
42. I. E. Batov, Yu. A. Nefyodov, M. R. Trunin, *et al.*, unpublished.
43. M. R. Trunin, Yu. A. Nefyodov, D. V. Shovkun, *et al.*, J. Supercond. (in press).
44. H. Enríquez, N. Bontemps, A. A. Zhukov, *et al.*, Phys. Rev. B (in press).
45. H. Kitano, T. Hanaguri, and A. Maeda, Phys. Rev. B **57**, 10946 (1998).
46. M. B. Gaifullin, Y. Matsuda, N. Chikumoto, *et al.*, Phys. Rev. Lett. **83**, 3928 (1999).

Translated by V. Sakun